

Article

# Opacity Corrections for Resonance Silver Lines in Nano-Material Laser-Induced Plasma

Ashraf M. EL Sherbini <sup>1</sup>, Ahmed H. EL Farash <sup>2</sup>, Tharwat M. EL Sherbini <sup>1</sup> and Christian G. Parigger <sup>3,\*</sup> 

<sup>1</sup> Laboratory of Laser and New Materials, Faculty of Science, Cairo University, Giza 12613, Egypt

<sup>2</sup> Engineering Physics Department, Military Technical College, Cairo 11766, Egypt

<sup>3</sup> Department of Physics and Astronomy, University of Tennessee, University of Tennessee Space Institute, Center for Laser Applications, 411 B. H. Goethert Parkway, Tullahoma, TN 37388, USA

\* Correspondence: cparigge@tennessee.edu; Tel.: +1-931-841-5690

Received: 21 June 2019; Accepted: 29 July 2019; Published: 31 July 2019



**Abstract:** Q-switched laser radiation at wavelengths of 355, 532, and 1064 nm from a Nd: YAG laser was used to generate plasma in laboratory air at the target surface made of nano-silver particles of size  $95 \pm 10$  nm. The emitted resonance spectra from the neutral silver at wavelengths of 327.9 nm and 338.2 nm indicate existence of self-reversal in addition to plasma self-absorption. Both lines were identified in emission spectra at different laser irradiation wavelengths with characteristic dips at the un-shifted central wavelengths. These dips are usually associated with self-reversal. Under similar conditions, plasmas at the corresponding bulk silver target were generated. The recorded emission spectra were compared to those obtained from the nano-material target. The comparisons confirm existence of self-reversal of resonance lines that emerge from plasmas produced at nano-material targets. This work suggests a method for recovery of the spectral line shapes and discusses practical examples. In addition, subsidiary calibration efforts that utilize the Balmer series H $\alpha$ -line reveal that other Ag I lines at 827.35 nm and 768.7 nm are optically thin under variety of experimental conditions and are well-suited as reference lines for measurement of the laser plasma electron density.

**Keywords:** laser-induced plasma; atomic spectroscopy; self-reversal; self-absorption; nanoparticles; silver; hydrogen

## 1. Introduction

Self-absorption as well as self-reversal of radiation from optically thick plasma occur due to processes of re-absorption in the outer-cooler region or in shockwave-induced density variations. The plasma produced by focusing of pulsed laser light on suitable targets suffers from strong inhomogeneity, even when using a well-defined TEM<sub>00</sub> laser mode [1]. Plasma inhomogeneities lead to strong gradients of plasma parameters (electron density and temperature) from the hot central core to peripheries that is in contact with surrounding air. This cooler plasma peripheries contain large population of atoms in lower atomic states, especially in the ground state. These peripheral atoms are often causing plasma re-absorption [2]. The plasma opacity manifests itself in form of homogeneous absorption of the spectral line that is labelled self-absorption. Effects of self-absorption include an apparent increase of the emitted line full-width at half-maximum (FWHM) and a decrease in spectral line height [3]. Line shape recovery is possible, only if one employs a standard, reliable measure of the true plasma electron density, which is offered by the optically thin H $\alpha$ - and H $\beta$ - lines [3,4], yet frequently the H $\alpha$ -line is utilized. For instance, line-of-sight measurements of laser-induced plasma at or near an ice surface [4,5] show self-reversal dips at the un-shifted resonance wavelength of the hydrogen alpha line of the Balmer series. Typical “fingerprints” due to re-absorption include

self-reversal and self-absorption [4–11]. In this work, self-absorption and self-reversal parameters, SR and SA, respectively, distinguish between these re-absorption effects.

There are significant challenges when considering self-reversed lines, especially for resonance lines, for the evaluation of the electron density measured from the full-width-at-half-maximum, and the determination of the temperature that is a function of the spectral radiance. Moreover, spectral line intensities from nano-based materials show differences from the corresponding bulk signals [12]. The theoretical descriptions of self-absorption and self-reversal [5–11] rely on the computation of the emitted radiation when modeling the emitters by a specific distribution.

However, strong enhanced plasma emission was noticed when focusing laser radiation onto targets made of pure nanomaterials [12–14]. This enhanced emission was related to the sudden increase of the population density of the ground state atoms in the same ratio of the amount of enhanced emission  $I_{\lambda_0}^{\text{Nano}}/I_{\lambda_0}^{\text{bulk}} \approx N_{\lambda_0}^{\text{Nano}}/N_{\lambda_0}^{\text{bulk}}$  [12–14], i.e., more of cold atoms,  $N_0^{\text{Nano}}$ , exist at the outer peripheries of plasma produced from nanomaterials [14], but without further increase in the plasma excitation temperature [2]. This enhanced emission enables the spectral line intensity  $I_{\lambda_0}^{\text{Nano}}$  of the resonance lines to exceed the corresponding, upper-limit black body radiation intensity  $I_{\lambda_0}^{\text{Nano}} \geq B(\lambda_0, T_{\text{ex}})$ ,

$$B(\lambda_0, T_{\text{ex}}) = \frac{2hc^2}{\lambda_0^5} \frac{1}{\exp\{hc/\lambda_0 k_B T_{\text{ex}}\} - 1} \quad (1)$$

because of the relatively local temperature,  $T_{\text{ex}}$ , in this plasma region. Therefore, and as elaborated by Fujimoto [2], i.e., the measured radiation intensities of the resonance lines are only those that emerge from the outer plasma regions at which the plasma optical depth is unity, hence self-reversal starts to act at the central un-shifted wavelengths of resonance lines that terminate at the ground state. Figure 1 illustrates a homogenized central core, cold periphery, the emanating “distorted” line shape and the upper limit of spectral intensity imposed by the black body radiation “tilted horizontal thick line”.

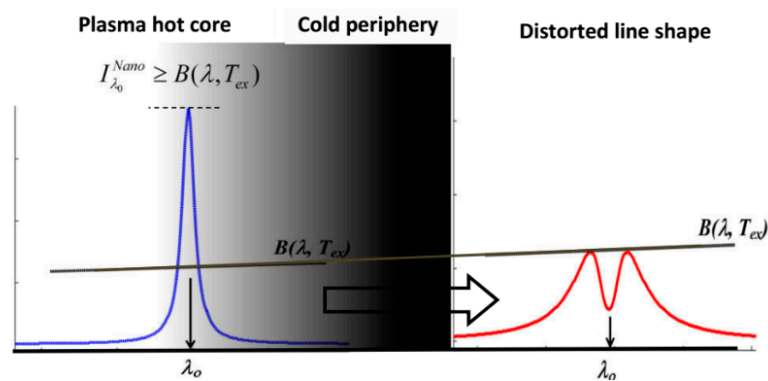


**Figure 1.** An illustration to the effect of plasma opacity on spectral line shape via self-reversal (red) in comparison to the undistorted shape (blue), together with the black body spectral intensity limit (black lines) for a specific excitation temperature at outer region of the plasma.

There are three effects that modify the line shape: First, the excessive enlargement of line FWHM; second, reduction of spectral radiance imposed by the black body radiation limit; and third, the reversal in the emitted line-shape.

This work introduces a method for retrieving the original undistorted shape of self-absorbed lines that are affected simultaneously by self-reversal and self-absorption. The method is based on the availability of certain optically-thin spectral lines that originate from upper states of atomic transitions, viz., Ag I lines at 827.35 and 768.7 nm. These Ag lines are investigated first by comparison of the determined electron density with that obtained from  $H_{\alpha}$ , and then serve as gauge for other optically-thick Ag lines.

## 2. Materials and Methods

In the experiments, an Nd:YAG laser device (Quantel model Brilliant B) operates at the fundamental wavelength of 1064 nm and the two harmonics at 532 and 355 nm, with output laser energy per pulses of  $370 \pm 5$ ,  $100 \pm 4$ , and  $30 \pm 3$  mJ, respectively. The corresponding spot sizes at the target surface amount to  $0.5 \pm 0.05$ ,  $0.44 \pm 0.05$ , and  $0.27 \pm 0.03$  mm. An optical fiber of 400  $\mu\text{m}$  diameter collects the radiation from the plasma. An echelle type spectrograph (SE200) with an average instrumental bandwidth of 0.12 nm, and an attached intensified charge-coupled device (Andor iStar DH734-18F) acquire the data. The spectral pixel resolution and pixel area amount to 0.02 nm and 196  $\mu\text{m}^2$ , respectively. A xyz-holder allows one to position the optical fiber at distance of 5 mm from the laser-induced plasma.

The time delay and gate width amount to 2  $\mu\text{s}$  for all experiments reported in this work. ICCD KestrelSpec<sup>®</sup> software subtracts the background stray light contributions. The measured electronic noise level amounts to  $20 \pm 7$  counts across wavelength range of 250–850 nm. The measurements of incident laser energy at each laser shot utilize a quartz beam splitter to direct the reflected part (4%) to a calibrated power-meter (Ophier model 1z02165). A 25 ps fast response photodiode in conjunction with digital storage CRO (type Tektronix model TDS 1012) measures the laser pulse width of  $5 \pm 1$  ns. A set of calibrated neutral density filters adjusts the energy/pulse. The DH2000-CAL lamp (Ocean Optics SN037990037) allowed us to correct for the sensitivity of detection system composed of spectrograph, intensified camera and optical fiber. A 500 kg/cm<sup>2</sup> press prepared the silver nanomaterial powder (from MKNANO<sup>®</sup>) to produce a less brittle tablet without further purification or heat treatments. The nanoparticle size equals  $95 \pm 10$  nm, as confirmed from measurements with a transmission electron microscope.

## 3. Results and Discussion

An example of the self-reversed resonance lines from the neutral silver atoms is presented in Figure 2 after laser irradiation with different wavelengths, namely, Figure 2a,d: 355 nm, Figure 2b,e: 532 nm, and Figure 2c,f: 1064 nm.

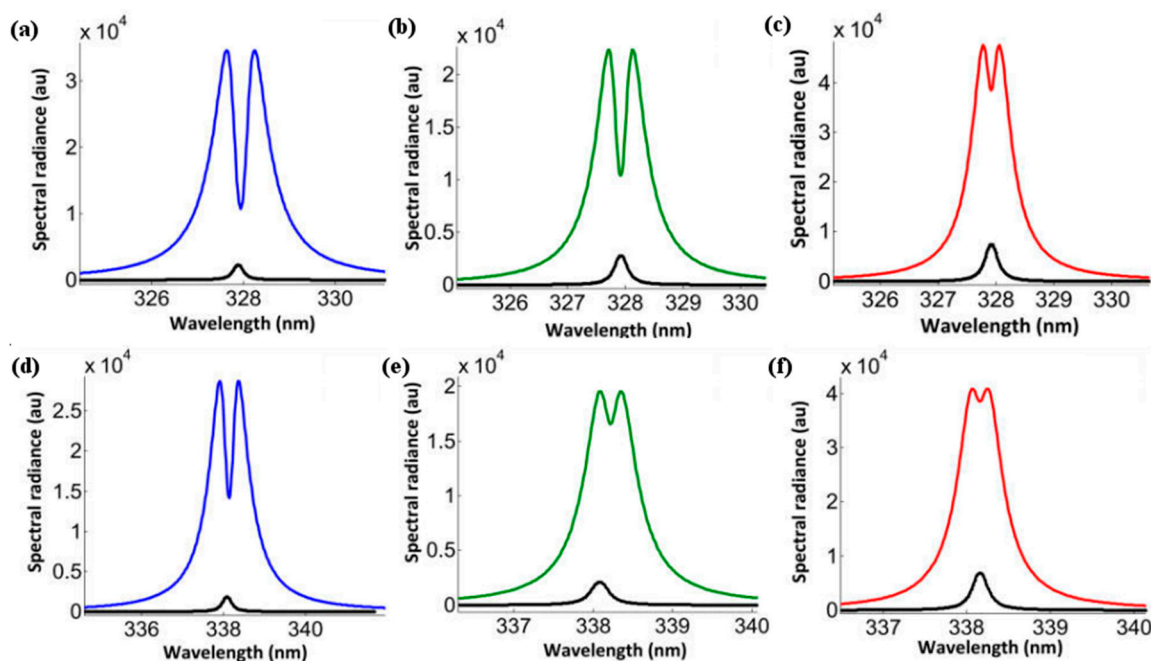


**Figure 2.** The effect of self-reversal on the resonance Ag I transition from nano-silver plasmas with respect to bulk target (black). Different laser irradiation wavelengths are indicated by different colors. (a,d) blue for 355 nm, (b,e) green for 532 nm, and (c,f) red for 1064 nm.

In Figure 2, the upper self-reversed spectral lines emerge from plasma generated at the surface of the nano-silver target. The lower black spectra are the corresponding lines for the same transition and under the same experimental conditions but from the bulk-silver target. One can notice significantly more self-reversal of the plasma created from nano-silver than for plasma from bulk-silver.

For the resonance transitions of the Ag I lines at 327.9 and 338.2 nm, Figures 3–5 illustrate recorded and fitted nano-material silver lines with central dips at line center.

The two sets of spectra show the results captured from nano-material silver targets with 355 nm radiation. The self-reversal of plasma radiation from nano-silver material is typically absent in investigations of laser-induced plasma with bulk-silver targets for otherwise similar experimental conditions. Figure 3 shows well-developed spectral dips. Accordingly, Figure 4 displays recorded spectra obtained with 532 nm harmonic laser excitation.

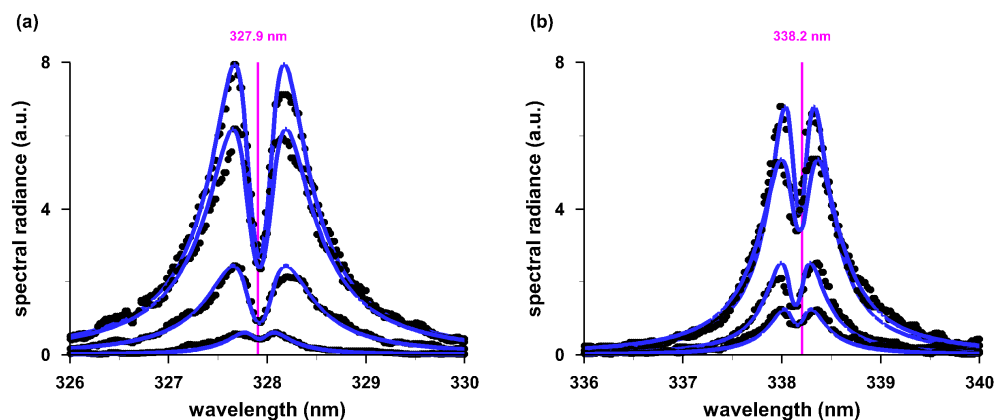


Figure 3. Ag I (a) 327.9 nm and (b) 338.2 nm lines, 355-nm excitation, fluences of 13.5, 9.6, 5 and 2.1 J/cm<sup>2</sup>.

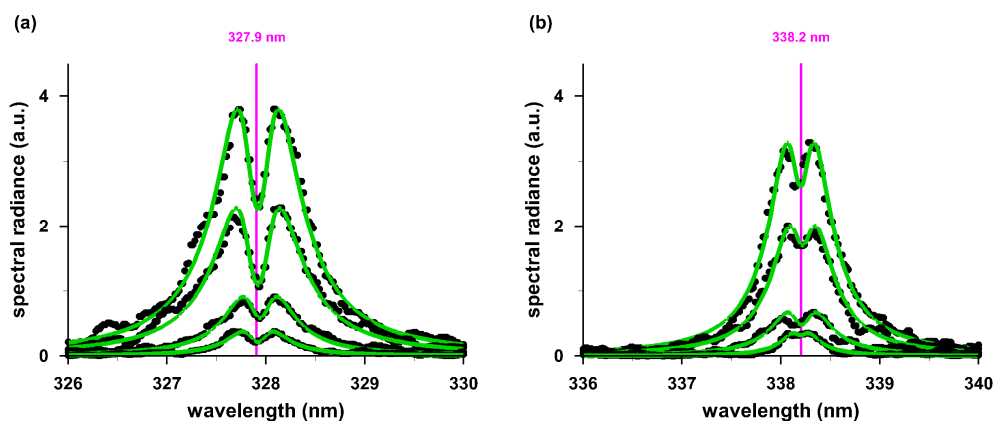
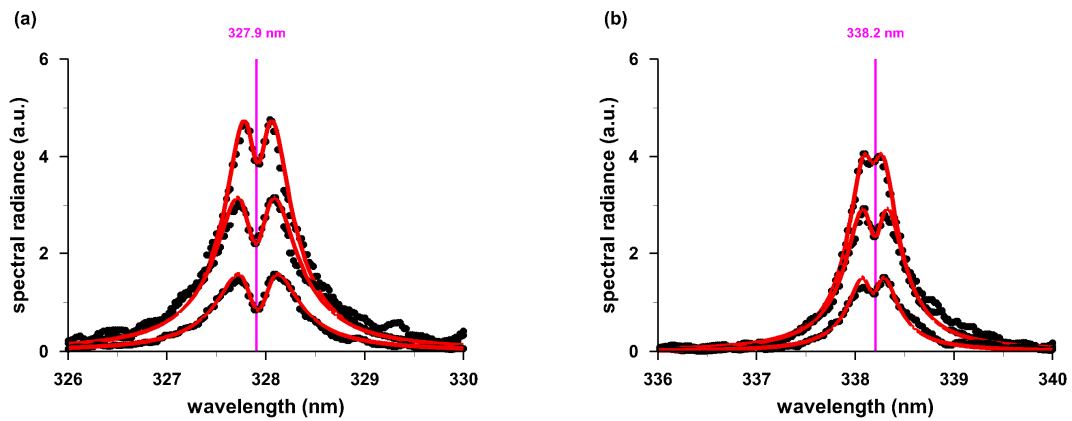


Figure 4. Ag I (a) 327.9 nm and (b) 338.2 nm lines, 532-nm excitation, fluences of 13.5, 11.5, 8, and 6 J/cm<sup>2</sup>.

Figure 4 indicates diminished self-absorption when compared to Figure 3. For 1064 nm laser excitation, Figure 5 displays even smaller self-absorption phenomena for the two silver lines.



**Figure 5.** AgI (a) 327.9 nm and (b) 338.2 nm lines, 1064-nm excitation, fluences of 13.5, 11.5, 8, and 6 J/cm<sup>2</sup>.

In view of Figures 3–5, one can see that it would be challenging to extract the full-width at half-maximum for determination of electron density. It would be required to extract the FWHM of the line after opacity corrections due to self-reversal and self-absorption effects.

An accurate electron-density measure of the nano-material plasma is required for the design of self-absorption correction procedures. The reliable H<sub>α</sub> line was supposed to provide a measure for electron density [3], but unfortunately, the H<sub>α</sub> line is absent when employing green and blue laser beams for plasma generation with nano-silver. Consequently, one needs to identify other suitable optically thin lines. In this work, opacity corrections for self-reversed and self-absorbed Ag lines are based on other optically-thin Ag lines.

In the process of locating suitable lines in place of H<sub>α</sub>, an extensive examination of emission spectral lines from the neutral silver discovers that only two Ag I lines at 827.35 or 768.7 nm are suitable candidates for reliable measurement of the ‘true’ electron density. The inferred electron densities compare nicely with the corresponding values obtained from analysis of the hydrogen alpha line of the Balmer series. Figure 6 illustrates the results, and Table 1 shows the comparisons.

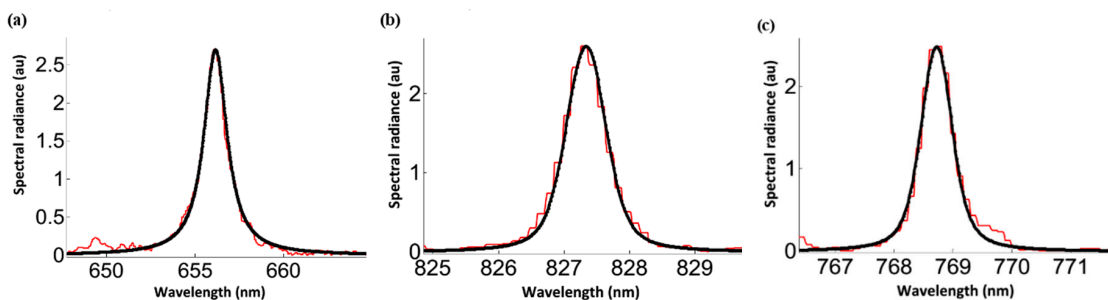


**Figure 6.** Recorded spectra for (a) H<sub>α</sub> at 656.28 nm, (b) Ag I at 827.35 nm, and (c) Ag I at 768.7 nm. Laser fluence 9.6 J/cm<sup>2</sup>, 1064-nm excitation.

**Table 1.** Electron densities, n<sub>e</sub>, in units of 10<sup>17</sup>cm<sup>-3</sup> for different fluence, 1064-nm excitation.

Laser Fluence (J/cm <sup>2</sup> )	n <sub>e</sub> : H <sub>α</sub> 656.28 nm	n <sub>e</sub> : Ag I 827.35 nm	n <sub>e</sub> : Ag I 768.7 nm
9.94	1.64	1.66	1.76
7.46	0.76	0.77	0.76
5.9	0.63	0.66	0.70
4.47	0.57	0.55	0.58

There is excellent agreement of the measured electron density from the H<sub>α</sub> and the two optically thin silver lines. The two silver lines Ag I at 827.35 and 768.7 nm are suitable for electron density

determination in nano- and bulk- material for the following reasons: First, the Ag lines emerge from the upper states  $4d^{10}6s-4d^{10}5p$  with almost empty lower and highly excited state  $4d^{10}6s$  that minimizes the possibility of plasma re-absorption by highly populated low atomic states. Second, both lines are observed in emission spectra of neutral silver under nearly all conditions.

The experimental evaluation included change of the incident laser fluence in the range from 5 to 10 J/cm<sup>2</sup> and measurement of the emission spectra during IR laser irradiation. The lines are Voigt-fitted to recorded spectral radiances as indicated by the solid black lines in Figure 6. The Stark broadening parameters for both lines are archived in Stark tables [15]: At the reference electron density of  $N_e^{ref} = 10^{17}$  cm<sup>-3</sup>, the Stark broadening parameter,  $\omega_S^{AgI}$ , amounts to  $\omega_S^{AgI} = 0.18 \pm 0.06$  nm. The Lorentzian components of the emitted lines,  $\lambda_S^{AgI}$ , were extracted. The electron densities listed in Table 1 were evaluated with the help of the expression,  $n_e^{AgI} \approx N_e^{ref} (\lambda_S^{AgI}/\omega_S^{AgI})$ , and then compared with the corresponding values obtained from H $\alpha$ .

For analysis of the self-absorbed spectra in Figure 2, notice line reversal at the center wavelength,  $\lambda_0$ , and weaker effects in the wings that lead to distortions. The transmittance [3,6],  $T(\tau_{\lambda_0})$ , is related to the escape factor [3,6] and it depends on the optical thickness of the plasma,  $\tau_{\lambda_0}$ .

The transmittance,  $T(\tau_{\lambda_0})$ , is modeled with a Lorentzian spectral line shape,  $\varphi(\lambda)$ ,

$$T(\tau_{\lambda_0}) = \int \varphi(\lambda)e^{-\tau_{\lambda_0} \varphi(\lambda)/\varphi_0} d\lambda, \quad \varphi(\lambda) = \frac{1}{\pi} \frac{0.5 \Delta\lambda_S}{(\lambda - \lambda_0)^2 + (0.5 \Delta\lambda_S)^2}, \quad (2)$$

where  $\Delta\lambda_S$  denotes the full-width at half-maximum (FWHM) of the normalized spectral line shape of magnitude  $\varphi_0$  at line center. The plasma optical thickness at line center,  $\tau_{\lambda_0}$ ,

$$\tau_{\lambda_0} = \int_{-\ell}^0 \kappa(\lambda_0) d\ell, \quad (3)$$

is defined in terms of integrated absorption coefficient,  $\kappa(\lambda)$ , of a spectral line measured along the line-of-sight,  $\ell$ , at the transition wavelength,  $\lambda_0$ . Figure 7 illustrates results for  $\tau_{\lambda_0}$  ranging from 0.25 to 2 at equal steps of 0.25, and for fixed Lorentzian FWHM of  $\Delta\lambda_S = 0.5$  nm. The line shape indicates a flat top for unity optical thickness, i.e.,  $\tau_{\lambda_0} = 1$ . For values higher than unity, self-absorption affects the line shape primarily at the center [2].

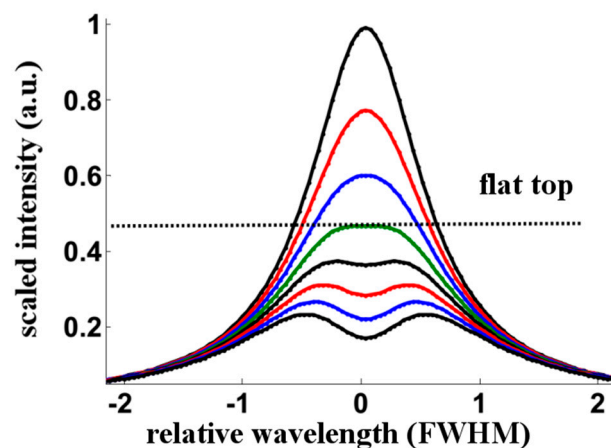


**Figure 7.** Line shapes  $\varphi(\lambda)e^{-\tau_{\lambda_0} \varphi(\lambda)/\varphi_0}$  vs. wavelength,  $\lambda$ , for fixed  $\Delta\lambda_S = 0.5$  nm. Values of  $\tau_{\lambda_0}$  range from 0.25 to 2.0 in steps of 0.25.

The fitting of the argument in Equation (2) to the experimentally measured line shape can be formulated with two line-shape parameters, namely, the self-absorbed Lorentzian FWHM,  $\Delta\lambda_{S1}$ , and the optical depth,  $\tau_{\lambda_0}$ , at line center [2].

The self-reversal parameter, SR, is introduced for a quantitative description of the measured line shapes. The parameter SR indicates the ratio of transmitted and of weakly ( $\kappa(\lambda) \ell \ll 1$ ) affected intensities at line center,

$$SR = \frac{1 - e^{-\tau_{\lambda_0}}}{\tau_{\lambda_0}} \leq 1, \tag{4}$$

or in terms of the transmittance,  $SR = T(\tau_{\lambda_0})$ . Self-reversal diminishes the peak spectral radiance as well. In comparison with self-absorption, self-reversal causes further apparent enlargement of the FWHM,  $\Delta\lambda_{S2}$ , with  $\Delta\lambda_{S2} > \Delta\lambda_{S1}$ . In analogy with the derivation of self-absorption [3], one can write  $\Delta\lambda_{S2} = \Delta\lambda_{S1} SR^\alpha$ . The value for the exponent is taken to be  $\alpha = -0.54$ , in analogy to previously reported self-absorption studies [3]. The self-reversal factor, SR, is functionally identical to that for the self-absorption factor [3], SA,  $\Delta\lambda = \Delta\lambda_{S0} SA^\alpha$ . Here,  $\Delta\lambda$  and  $\Delta\lambda_{S0}$  indicate the FWHM of spectral lines with and without self-absorption, respectively.

Figure 8 summarizes two typical examples of the discussed spectral line shape analysis for the measured Ag I lines at 327.9 and 338.2 nm. Figure 8a,d display self-reversed data, Figure 8b,e portray corrected lines that are still self-absorbed, and Figure 8c,f illustrate the retrieved line-shapes when using data from the optically thin line at 827 nm.

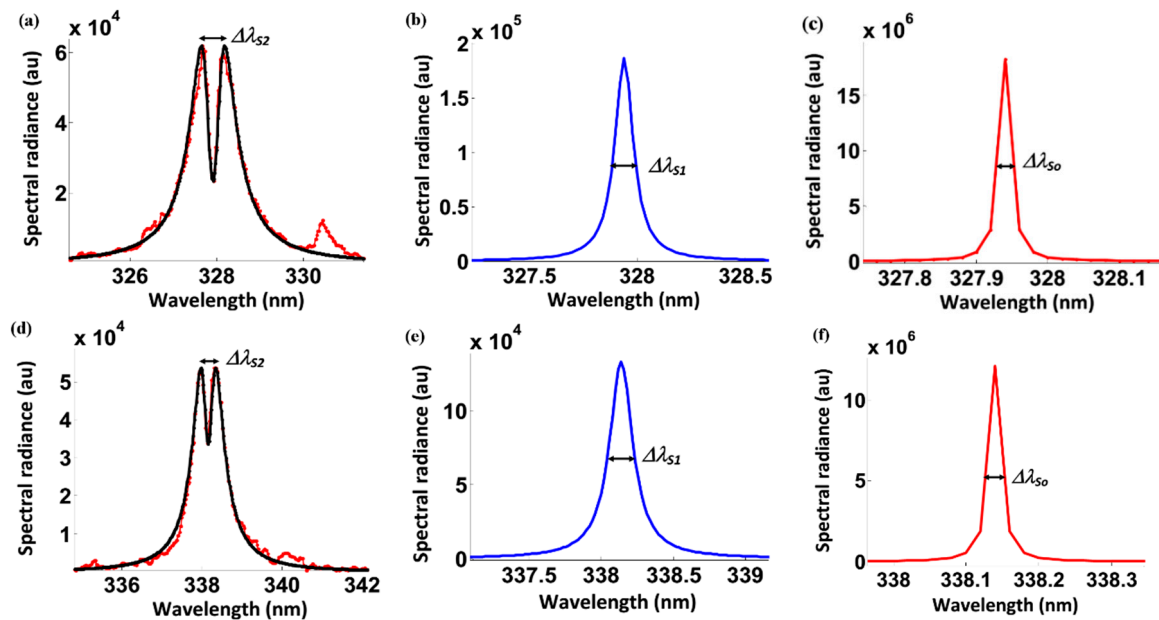


**Figure 8.** Line shapes (a) self-reversed  $\Delta\lambda_{S2} = 0.37$  nm,  $SR = 0.3$ ,  $T(\lambda) = 33\%$ ; (b) Self-absorbed  $\Delta\lambda_{S1} = 0.2$  nm,  $n_{e1} = 4.2 \times 10^{18} \text{ cm}^{-3}$ ,  $SA = 0.01$ ; (c) Reconstructed 327.9-nm optically thin line:  $\Delta\lambda_{S0} = 0.017$  nm,  $n_{e1} = 3.5 \times 10^{17} \text{ cm}^{-3}$ ,  $SA = 1$ . (d)  $\Delta\lambda_{S2} = 0.32$  nm,  $SR = 0.38$ ,  $T(\lambda) = 40\%$ , (e)  $\Delta\lambda_{S1} = 0.19$  nm,  $SA = 0.01$ , and (f) 338.2-nm line:  $\Delta\lambda_{S0} = 0.017$  nm,  $n_{e1} = 3.5 \times 10^{17} \text{ cm}^{-3}$ ,  $SA = 1$ . Light pulses for (a,d) of fluence  $13.5 \text{ J/cm}^2$  at 355 nm generated laser plasma. Reconstruction for (c,f) is accomplished with data from the 827-nm line.

The measured widths and plasma transmission percentages (typically 33% and 40% for the reported experiments) are included in the figure captions. The theoretical, asymptotic form for the transmittance of a Lorentzian line profile [2,6] equals

$$T_{\text{theory}}(\tau_{SR}) \sim 1 / \sqrt{\pi \tau_{SR}} \tag{5}$$

The theoretical transmittances are compatible with SR factors of 0.32 and 0.38. The measured line shapes are well-described by the fitted Lorentzians. However, for sake of simplicity, this discussion omits Gaussian components due to instrumental broadening of  $\Delta\lambda_{\text{instrument}} \sim 0.12$  nm. Figure 8a,d

show a significant reduction in intensity along with an apparent increase in broadening ( $\Delta\lambda_{S2}$ ). The self-reversal coefficients are relatively small (SR = 0.32 and SR = 0.38), but due to line center effects [2,5–10] dips occur. Noteworthy in this work, self-reversal (quantified by the coefficient SR) is almost independent of the laser fluence, but self-absorption (SA) changes monotonically with laser fluence.

In this example, the self-reversal peak separation provides values for  $\Delta\lambda_{S2}$ , using the FWHM of lines with the dip would cause even larger discrepancies for the electron density,  $n_e$ . From Equation (5), computed  $\Delta\lambda_{S1}$  would show electron densities that are ~ ten times higher than obtained from the optically thin line that was retrieved by comparison with 827-nm results. When using lower fluence levels for these two lines, larger variances occur in inferred  $n_e$  values. From  $\Delta\lambda = \Delta\lambda_{S0} SA^\alpha$ , a factor of ten higher electron density means that the self-absorption factor is of the order of  $SA \sim 0.01$ . For self-absorption, the magnitude of the peak spectral irradiances can be evaluated [3] using  $I_0(\lambda_0) \sim I_1(\lambda_0)/SA$ , leading to two orders of magnitude higher irradiances. Such discrepancy indicates significant self-absorption and line reversal for the selected example.

#### 4. Conclusions

Self-absorption may lead to a decrease in the peak line intensity up to two orders of magnitude, including appearance of self-reversed lines. Even after taking into consideration the line shape effects, occurrence of self-absorption for a measured line contraindicates plasma electron density and temperature measurements from that line. The experimentally measured transmission factors for the 327.9 and 338.2 nm lines change with incident laser fluence. The theoretical analysis predicts transmittance values consistent with the measured ones within the experimental margins of error. The optically thin, 827-nm silver line allows one to determine the electron density showing decreases as expected from  $3.5 \times 10^{17}$  to  $1.1 \times 10^{16} \text{ cm}^{-3}$  with decreasing laser fluence. However, as self-absorption of the silver 338.2 nm line decreases with decreasing fluence, the variations of inferred electron densities are larger than anticipated, or the 338.2 nm line shows a larger standard deviation than the 827 nm line. The Ag I line at 338.2 nm disappears for a laser fluence of  $2.1 \text{ J/cm}^2$ . Finally, plasma opacity manifests itself as a combination of self-absorption and self-reversal effects, and line recovery would require results from an optically thin line, or in other words, self-absorbed or self-reversed lines are ill-suited as electron density diagnostic of laser plasma.

**Author Contributions:** A.M.E.S. conceived and performed the experiments. A.M.E.S. analyzed the result together with C.G.P., and all authors contributed to the writing of the article.

**Funding:** This research received no external funding.

**Conflicts of Interest:** The authors declare no conflict of interest.

#### References

1. Eidmann, K.; Sigel, R. Second-Harmonic Generation in an Inhomogeneous Laser-Produced Plasma. *Phys. Rev. Lett.* **1975**, *34*, 799–802. [[CrossRef](#)]
2. Fujimoto, T. *Plasma Spectroscopy*; Clarendon Press: Oxford, UK, 2004.
3. El Sherbini, A.M.; El Sherbini, T.M.; Hegazy, H.; Cristoforetti, G.; Legnaioli, S.; Palleschi, V.; Pardini, L.; Salvetti, A.; Tognoni, E. Evaluation of self-absorption coefficients of aluminum emission lines in laser-induced breakdown spectroscopy measurements. *Spectrochim. Acta Part B At. Spectrosc.* **2005**, *60*, 1573–1579. [[CrossRef](#)]
4. Parigger, C.G.; Surmick, D.M.; Gautam, G.; El Sherbini, A.M. Hydrogen alpha laser ablation plasma diagnostic. *Opt. Lett.* **2015**, *40*, 3436–3439. [[CrossRef](#)] [[PubMed](#)]
5. Parigger, C.G.; Surmick, D.M.; Gautam, G. Self-absorption characteristics of measured laser-induced line shapes. *J. Phys. Conf. Ser.* **2017**, *810*, 012012. [[CrossRef](#)]
6. Irons, F.E. The escape factor in plasma spectroscopy—I. The escape factor defined and evaluated. *J. Quant. Spectrosc. Radiat. Transf.* **1979**, *22*, 1–20. [[CrossRef](#)]
7. Holstein, T. Imprisonment of Resonance Radiation in Gases. *Phys. Rev.* **1947**, *72*, 1212–1232. [[CrossRef](#)]

8. Holstein, T. Imprisonment of Resonance Radiation in Gases. II. *Phys. Rev.* **1951**, *83*, 1159–1168. [[CrossRef](#)]
9. Cowan, R.D.; Dieke, G.H. Self-Absorption of Spectrum Lines. *Rev. Mod. Phys.* **1948**, *20*, 418–455. [[CrossRef](#)]
10. Kielkopf, J.F.; Allard, N.F. Shift and width of the Balmer series H $\alpha$  line at high electron density in a laser-produced plasma. *J. Phys. B At. Mol. Opt. Phys.* **2014**, *47*, 155701. [[CrossRef](#)]
11. Moon, H.-Y.; Herrera, K.K.; Omenetto, N.; Smith, B.W.; Winefordner, J.D. On the usefulness of a duplicating mirror to evaluate self-absorption effects in laser induced breakdown spectroscopy. *Spectrochim. Acta Part B At. Spectrosc.* **2009**, *64*, 702–713. [[CrossRef](#)]
12. EL Sherbini, A.M.; Parigger, C.G. Wavelength dependency and threshold measurements for nanoparticle-enhanced laser-induced breakdown spectroscopy. *Spectrochim. Acta Part B At. Spectrosc.* **2016**, *116*, 8–15. [[CrossRef](#)]
13. EL Sherbini, A.M.; Parigger, C.G. Nano-material size dependent laser-plasma thresholds. *Spectrochim. Acta Part B At. Spectrosc.* **2016**, *124*, 79–81. [[CrossRef](#)]
14. El Sherbini, A.M.; Hagrass, M.M.; Rizk, M.R.M.; El-Badaway, E.A. Plasma ignition threshold disparity between silver nanoparticle-based target and bulk silver target at different laser wavelengths. *Plasma Sci. Technol.* **2019**, *21*, 015502. [[CrossRef](#)]
15. Dimitrijević, M.S.; Sahal-Bréchet, S. Stark broadening of Ag I spectral lines. *At. Data Nucl. Data Tables* **2003**, *85*, 269–290. [[CrossRef](#)]



© 2019 by the authors. Licensee MDPI, Basel, Switzerland. This article is an open access article distributed under the terms and conditions of the Creative Commons Attribution (CC BY) license (<http://creativecommons.org/licenses/by/4.0/>).